Regional geomorphology and history of Titan's Xanadu province

J. Radebaugh [a], R.D. Lorenz [b], S.D. Wall [c], R.L. Kirk [d], C.A. Wood [e], J.I. Lunine [f], E.R. Stofan [g], R.M.C. Lopes [c], P. Valora [a], T.G. Farr [c], A. Hayes [h], B. Stiles [c], G. Mitri [c], H. Zebker [i], M. Janssen [c], L. Wye [i], A. LeGall [c], K.L. Mitchell [c], F. Paganelli [g], R.D. West [c], E.L. Schaller [j], The Cassini Radar Team

[a] Department of Geological Sciences, Brigham Young University, S-389 ESC Provo, UT 84602, United States
[b] Johns Hopkins Applied Physics Laboratory, Laurel, MD 20723, United States
[c] Jet Propulsion Laboratory, California Institute of Technology, 4800 Oak Grove Drive, Pasadena, CA 91109, United States
[d] US Geological Survey, Branch of Astrogeology, Flagstaff, AZ 86001, United States
[e] Wheeling Jesuit University, Wheeling, WV 26003, United States
[f] Department of Physics, University of Rome "Tor Vergata", Rome 00133, Italy
[g] Proxemy Research, P.O. Box 338, Rectortown, VA 20140, USA
[h] Department of Geological Sciences, California Institute of Technology, Pasadena, CA 91125, USA
[i] Department of Electrical Engineering, Stanford University, 350 Serra Mall, Stanford, CA 94305, USA
[j] Lunar and Planetary Laboratory, University of Arizona, Tucson, AZ 85721, USA

ARTICLE INFO

ABSTRACT

Titan's enigmatic Xanadu province has been seen in some detail with instruments from the Cassini spacecraft. The region contains some of the most rugged, mountainous terrain on Titan, with relief over 2000 m. Xanadu contains evolved and integrated river channels, impact craters, and dry basins filled with smooth, radar-dark material, perhaps sediments from past lake beds. Arcuate and aligned mountain chains give evidence of compressional tectonism, yet the overall elevation of Xanadu is puzzlingly low compared to surrounding sand seas. Lineations associated with mountain fronts and valley floors give evidence of extension that probably contributed to this regional lowering. Several locations on Xanadu's western and southern margins contain flow-like features that may be cryovolcanic in origin, perhaps ascended from lithospheric faults related to regional downdropping late in its history. Radiometry and scatterometry observations are consistent with a water–ice or water–ammonia–ice composition to its exposed, eroded, fractured bedrock; both microwave and visible to near-infrared (v-nIR) data indicate a thin overcoating of organics, likely derived from the atmosphere. We suggest Xanadu is one of the oldest terrains on Titan and that its origin and evolution have been controlled and shaped by compressional and then extensional tectonism in the icy crust and ongoing erosion by methane rainfall.

1. Introduction

Xanadu, the first surface feature of Titan seen from Earth (Lemmon et al., 1993; Smith et al., 1996), stands out globally as a bright feature on Titan's leading hemisphere (centered on the equator and ~100°W longitude) as seen in the near-IR (n-IR). This brightness is the result of either compositional or textural differences in this region compared with other areas on Titan. Xanadu is a land of extremes, boasting the longest and most well-developed river channels, the highest mountains, the widest valleys, and the most candidate impact craters of any region on Titan.

We describe the regional geomorphology of Xanadu in the context of other regions around Titan, mainly as seen by the Cassini spacecraft's synthetic-aperture radar (SAR). An understanding of

the formation and evolution of Xanadu will help us to understand processes on Titan's surface and in its interior.

1.1. Discovery of Xanadu

Although Xanadu was retroactively detected (Richardson et al., 2004) in Voyager-1 optical (orange filter ~0.65 μm) images acquired in 1980, the first indications in the n-IR lightcurve of a distinct leading-face terrain on Titan were published by Lemmon et al. (1993) and Noll and Knacke (1993). These n-IR data showed that at several methane-window wavelengths (e.g. 1.1, 1.3 and 1.6 μm), Titan's leading face was a few to a few tens of percent brighter than the longitudinal average. Further studies (Lemmon et al., 1995) indicated that the lightcurve might be fitted by a large bright region centered at 90°W longitude, with a second large bright region further to the east.

Xanadu was the most prominent feature in the first nIR maps of Titan made with images acquired with the refurbished Hubble

Corresponding author. Fax: +1 801 422 0267.
E-mail address: jani.radebaugh@byu.edu (J. Radebaugh).

Space Telescope (HST) in 1994. The feature was evident in maps made in the 0.94 and 1.08 μm CH$_4$ windows, and its western edge was apparent at 0.67 μm (Smith et al., 1996). The images used to make the maps had a resolution of ~300 km, and Xanadu (known as the "leading-edge bright feature" until its name approval by the IAU in 2004) was identified as having a size of 4000 × 2500 km. Xanadu was the feature typically reported as a benchmark in the development of various groundbased adaptive optics systems in the decade around 2000, and was clearly seen in maps made with other HST data (Meier et al., 2000).

Combes et al. (1997) noted that Xanadu appeared to contain two or more spots brighter than the rest of the feature in adaptive optics images at 1.3 and 1.6 μm wavelength. However, some caution in assigning significance to these regions is warranted, since clouds and/or seasonal variations in stratospheric haze can vary the apparent brightness at a given location, either by adding scattered light directly or by obscuring the surface reflection beneath. There are some hints of these brighter regions in shorter-wavelength (0.94 μm) imagery around the same epoch (Smith et al., 1996), although they are not obvious in the Cassini ISS (Imaging Science Subsystem, v-nIR camera) map at the same wavelength acquired in 2004 (Porco et al., 2005).

Titan's leading face, and Xanadu in particular, is also bright to groundbased radar. A disk-integrated 12-cm radar lightcurve (opposite circular polarization) obtained at Arecibo by Campbell et al. (2003) mirrors the n-IR lightcurve closely, peaking at 90°W longitude. Xanadu is also bright to Cassini SAR, as will be described in Section 2.

1.2. Location and extent of Xanadu

The boundaries of Xanadu have not been formally defined, in part because terrain around it has not been completely observed or mapped, and also because boundaries perceived at different wavelengths are not always coincident. Although some transitions, such as those between bright mottled and dark dune or bright mountain and dark lowland terrains, are sharp, other boundaries are diffuse and yet must represent a change from terrain we label as part of Xanadu and other regions with distinctly different characteristics. Here we specify a polygonal set of boundaries for Xanadu to define the area discussed and to serve as an algorithmic specification for future radiometric and altimetric studies (Fig. 1).

The transition between western Xanadu and the Shangri-La terrain west of Xanadu consists of moderately SAR-bright, mottled terrains of western Xanadu grading rather abruptly to the SAR-dark dune seas of Shangri-La. The boundary is moderately sharp (and indeed has been used as a feature to correlate HST and Voyager data to constrain Titan's rotation rate – e.g. Richardson et al., 2004). This edge maintains an azimuth of about N 45°E from the location 15°S, 150°W to 15°N, 120°W (Fig. 1). This margin is also sharp optically, as seen by ISS (Fig. 1; Porco et al., 2005), but comparison of ISS and SAR images reveals that the sharp boundaries in the two wavelength ranges, though often well correlated, are not universally so (Kirk et al., 2006). The v-nIR bright region of Xanadu contains some SAR-dark but mostly SAR-bright terrains.

The northern edge of Xanadu is a zone of transition between SAR-bright (and radar scatterometry-bright, see Section 4) mountainous terrain and SAR-dark materials, either dune fields or bland lowlands. This boundary nearly coincides with the 15th parallel, so for simplicity we consider this as the northern edge of Xanadu, although some bright material extends farther north at ~120°W. The eastern and northeastern edges of Xanadu consist of a transition between SAR-bright, mountainous terrain and SAR-dark, bland lowlands. Many bands of mountainous regions grade eastwards into the lowlands, making a strict boundary definition difficult. We choose the fairly distinct bright-dark boundary defined by

the dark 'H' of Fensal-Aztlan, at ~50°W longitude to be Xanadu's eastern margin (Fig. 1).

As we discuss in this paper, the geology around the southern edge of Xanadu is complex. We suggest the spectrally anomalous regions Tui Regio and Hotei Arcus reside just within Xanadu's borders because this leads to a geometrically simpler boundary, their SAR brightness is consistent with that of western Xanadu, and their histories mesh well with Xanadu's model history described below. To accommodate these distinctions, we adopt the 30th south parallel as the southern boundary of Xanadu, between the longitudes 120°W and 75°W (Fig. 1). Xanadu's southeastern boundary links the southern margin from the western apex of the Atzlan dark region at 20°S, 60°W to the eastern apex of Xanadu at 10°S, 45°W encompassing Hotei Arcus and defining a boundary between Xanadu and the (radiometrically similar) Tsegihi terrain to the southeast.

In summary, the coordinates (10°S, 45°W; 30°S, 75°W; 30°S, 120°W; 15°S, 150°W; 15°N, 120°W; 15°N, 90°W; 10°S, 45°W) define a polygon that we consider here to be Xanadu. These boundaries are certain to change as we obtain more data and understanding about Xanadu's origin and history, but for this regional, morphological study, this polygon is adequate.

2. Cassini observations of Xanadu

The Cassini spacecraft has been orbiting and observing Saturn and its family of rings and icy moons since 2004. Observations made by the v-nIR instruments ISS and VIMS (Visual and Infrared Mapping Spectrometer) have distinguished Xanadu from surrounding terrains, mainly in terms of v-nIR brightness (Barnes et al., 2005; Fig. 1). Additionally, VIMS has noted an association between mountainous regions on the eastern end of Xanadu and the VIMS "dark blue" unit, indicating a higher proportion of exposed water ice than the average for Titan (Barnes et al., 2007; throughout this paper, color designations of VIMS-derived units are those used by Soderblom et al. (2007). Their "dark blue" unit appears as such in any of several false-color presentations in which the 1.3 μm band is mapped to the blue channel).

The Cassini Titan Radar Mapper (hereafter Cassini RADAR) has obtained SAR at several locations within Xanadu. Cassini RADAR acquires data in SAR, scatterometry, radiometry (natural emission) and altimetry modes; variations on the SAR technique result in high-altitude, lower resolution SAR ("HiSAR") and SAR-derived topography ("SARTopo", Stiles et al., 2009). All observations are obtained at Ku-band (λ = 2.17 cm, f = 13.78 GHz). A SAR swath 120–450 km wide and up to several thousand kilometers long is created from five antenna beams (Elachi et al., 2005) displaying backscattered radiation at a resolution varying from 300 m to 1 km, depending on spacecraft range and orbital geometry. By the end of the Cassini Extended Mission (XM), 33 Titan SAR image swaths were obtained over a range of latitudes and longitudes (dominantly equatorial and north polar, leading hemisphere), covering nearly 40% of Titan's surface. Five of these SAR image swaths (T13, T41, T43, T44, and T48) and three HiSAR images (T20, T41, and T43) cover portions of Xanadu (Fig. 2). T13 (obtained on 30 April 2006) covers the central portion and extends across its west and east boundaries. Xanadu's southern margin is nearly outlined by the northern boundary of the T41 swath (obtained 22 February 2008). T48 lies just north of T41, on top of the T43 hiSAR image, but ends near the western boundary. Both T43 (obtained 12 May 2008) and T44 (obtained 28 May 2008) take a NW–SE track across the west-central portion of Xanadu, crossing its northern boundary (Fig. 2).

High SAR image brightness results from surfaces that are rough or fractured at the wavelength scale, are facing towards the instru-
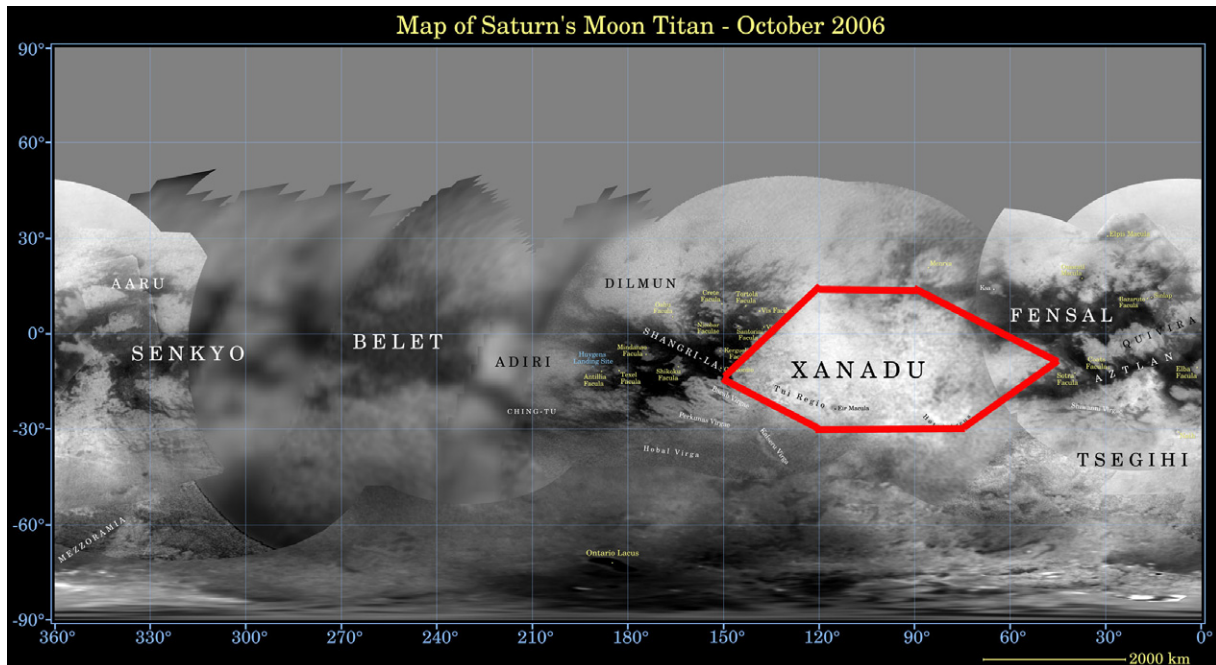
Fig. 1. Regional location of Xanadu with boundaries outlined in red. Azimuths and endpoints of each polygon segment are described in Section 1.2. The underlying basemap is a Cassini ISS image mosaic produced in 2006, see http://www.photojournal.jpl.nasa.gov/catalog/PIA08346. (For interpretation of the references to color in this figure legend, the reader is referred to the web version of this article.)
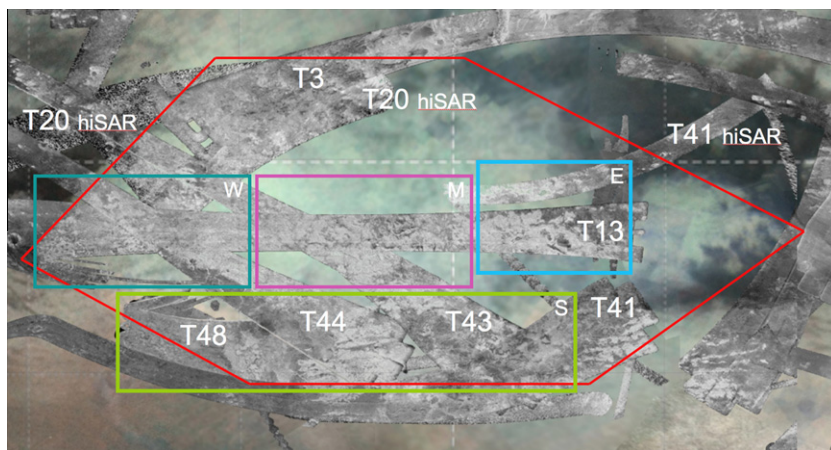

Fig. 2. Cassini Radar SAR image swaths covering the Xanadu region. The T3, T13, T41, T43, T44, and T48 swaths are labeled, with HiSAR from the T20 and T41 observations (all described in Section 2). This image stretches from 40°S to 10°N latitude and 70–170°W longitude. The underlying basemap is a combination of VIMS and ISS images, http://www.photojournal.jpl.nasa.gov/target/Titan. Major regional divisions of Xanadu are delineated by four boxes. W is the Western Drainages, M is the Middle Rugged Terrains, E is the Eastern Belts, and S is the Southern Flow Complexes. Each division is described in detail in Section 3.

ment, or have high intrinsic reflectivity at the pixel scale. Low image brightness comes from surfaces that are signal-absorbing, smooth, or slope away from the instrument (Cassini SAR incidence angles range from ~15° to 40°). Microwaves can also penetrate and scatter within materials to enhance image brightness; this effect is termed volume scattering (e.g., Ulaby and Fung, 1981), and is believed to be particularly important for Xanadu (Janssen et al., 2009). Although some features can appear quite different when viewed from different geometries (e.g., Blom, 1988), much of Xanadu is bright to SAR as seen from a range of incidence angles.

Scatterometry, radiometry (measurement of natural thermal emission) and altimetry measurements of Xanadu were also obtained by Cassini RADAR at greater range from Titan than SAR images. In these modes, Xanadu has a higher backscatter and lower brightness temperature than most other regions on Titan. Details of these observations are discussed in Section 4.

Xanadu is home to large regions of rugged, fractured, mountainous terrains as well as materials that have wavelength-scale texture and inherently high microwave reflectance (Janssen et al., submitted for publication). Together, these effects result in the highest signals returned to SAR from Titan. The geology of these terrains is discussed in the following section.

3. Geology and morphology of Xanadu

Though large and diverse, Xanadu can be divided into four major areas, according to location and morphological distinctions. Their names refer to dominant landforms in the region, to facilitate discussion and recall, but they are not map units, as in the style of other planetary geologic maps (see e.g. maps for regions of Io by Williams et al. (2002)). These areas are the Western Drainages,

the Middle Rugged Terrains, the Eastern Belts, and the Southern Flow Complexes, and are described below. We analyze the morphologies of these regions in order to understand their geologic origins and histories, and thus the history of Xanadu as a whole.

3.1. Western Drainages

The western portion of Xanadu, stretching from ~150° to 130°W longitude, is characterized overall by subdued topography, with relief likely of less than a few hundred meters based on SAR-shadow analysis and basic radarclinometry and stereo (described in Section 3.2). Because the SAR images do not show evidence of (bright or dark) shading at the margin of Xanadu that would be expected if locally steep slopes were present, we conclude that the western margin does not appear to differ much in elevation from the sand sea Shangri-La to the west (Kirk et al., submitted for publication; Fig. 3a). As discussed in Porco et al. (2005), the western boundary of bright Xanadu and dark Shangri-La is optically quite sharp (Fig. 1). Radar data also indicate a difference in brightness between the margin of Xanadu and the adjacent dune-dominated area, nearly as distinct as in the optical. The terrain at Xanadu's western edge is dark and has a mottled texture to SAR, with intermingled bright and dark lobate features (Fig 3a; Wall et al., 2009).

East of these lobate materials are areas that appear to be elevated above the margins (Lopes et al., 2010). They have a brighter appearance to SAR, with some bright/dark shading indicative of mountains and valleys (Kirk et al., 2005; Radebaugh et al., 2007). There are plateau-like features raised above surrounding terrains by ~100 m or less with stream channels carved into their surfaces (Fig. 3c). Many of these stream channels are of at least order three as visible at SAR resolutions. They are some of the most well-developed channels seen on Titan. (Lorenz et al., 2008; Baugh, 2008; Burr et al., 2009; Malaska et al., 2010). They are most likely formed by methane rainfall (Lorenz et al., 2008), can be traced for 200 km and may extend farther (Fig 3b and d). Based on the convergence angles of the network links and the elongation of the whole network, the assumed gradient at the time of formation is southward (Burr et al., 2009; Fig 3b and d). The study of Burr et al. (2009) revealed that the network is rectangular, with tributaries that indicate an east–west tectonic fabric, in addition to the regional
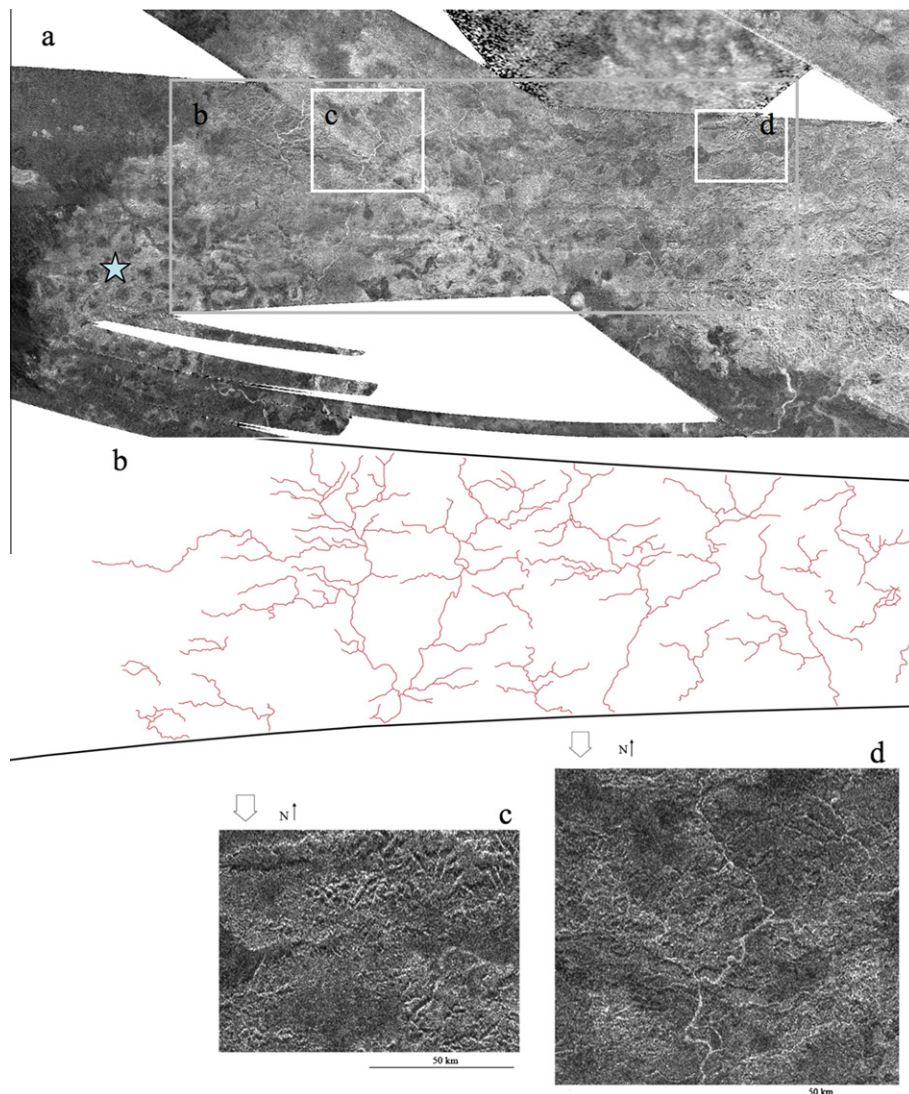

Fig. 3. (a) SAR observations of the Western Drainages region. Mostly lobate, arcuate materials on the western margin are intermingled with slightly elevated materials carved by extensive river systems. Boxes indicate location of figures (b)–(d). Star in the west indicates VIMS 5-μm bright region, discussed in Section 3. (b) Outlines of river channels seen in (a). Dendritic pattern indicates a gentle regional southward gradient. (c) Elevated plateaus seen in the northeast area of the Western Drainages. (d) Tributary system and main trunk of a Xanadu river. The meandering morphology indicates a low gradient.

southward gradient. The southward drainage trend is persistent across Xanadu, as described below.

3.2. Middle Rugged Terrains

The middle region of Xanadu, stretching from ~130° to 110°W longitude, is characterized by extremely rugged and elevated topography (Fig. 4). There are many adjacent mountain peaks, some of which are the highest relief measured on Titan – over 2000 m (Fig. 4b; Radebaugh et al., 2007; Lopes et al., 2010). These mountainous regions occur in blocks of roughly 50 km across and are surrounded by aureoles of SAR-bright materials that may have been eroded from the mountain tops or are pediment-like erosional features.

Between the mountain patches are regions dark to SAR, composed of smooth or microwave-absorbing materials. These roughly follow enlarged drainage patterns, similar in morphology to drowned river valleys such as the Chesapeake Bay (US, Maryland and Virginia) or Lake Powell, (US, Utah). In the eastern portion of the Middle Rugged Terrains these dark, enlarged valleys become more closely spaced and darker to SAR. These dark areas return some microwave signal above the instrument noise, and are therefore not nearly as dark as the north polar lakes (Stofan et al., 2007). Thus, we think these valleys are not filled with liquid, but instead with solid materials smooth or mostly absorbing to microwaves. These materials could have been eroded from surrounding peaks or brought to these locations by other processes, then carried and deposited by fluvial or lacustrine processes. Thus, better terrestrial analogs may be the Basin and Range province of the western US, where materials have been eroded from surrounding peaks and carried and deposited into intervening valleys, and the Po River Valley in northern Italy, where sediments produced by
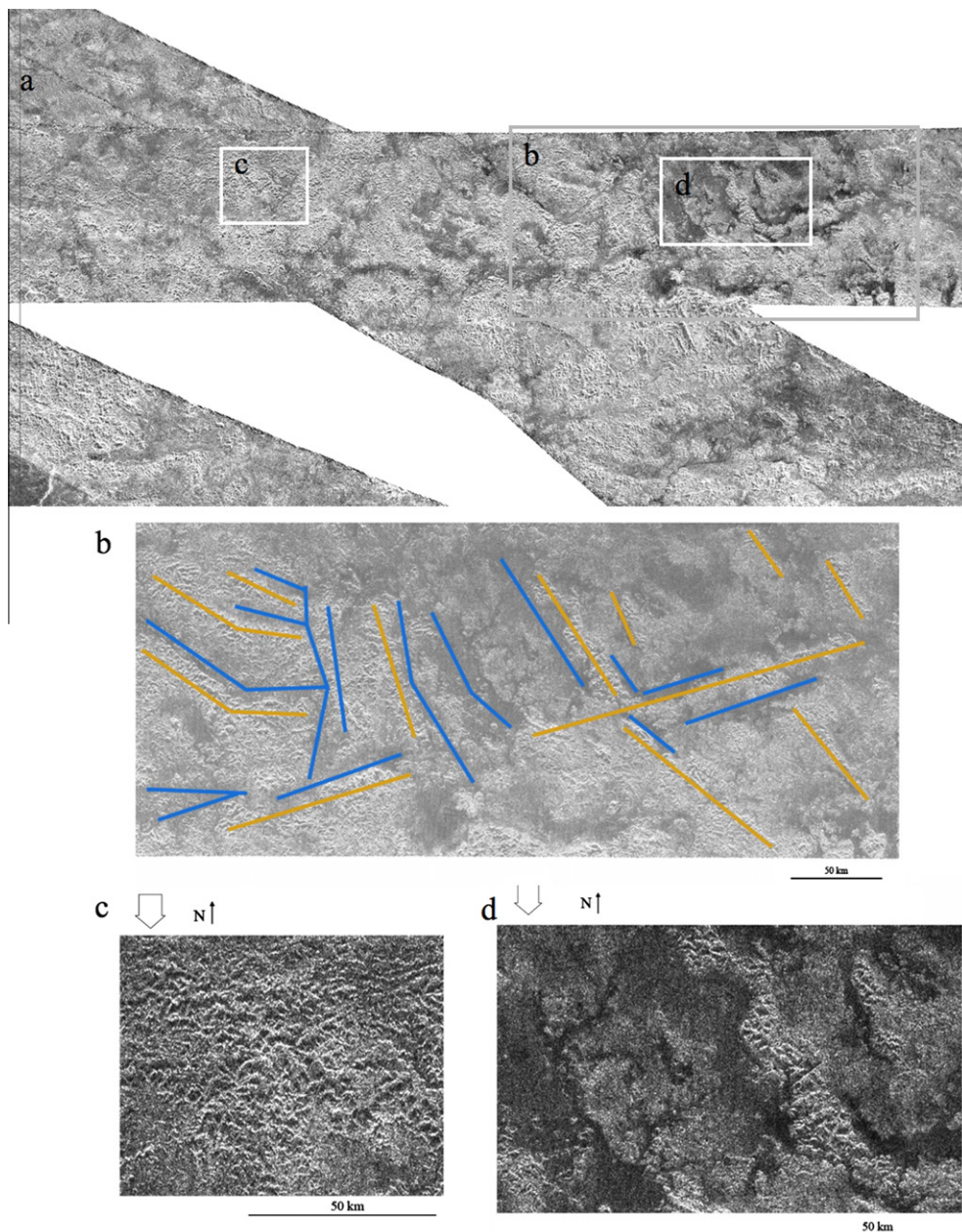

Fig. 4. (a) SAR observations of the Middle Rugged Terrains, consisting of closely spaced mountain peaks interspersed with broad, dark valleys. Boxes indicate locations of figures (b)–(d). (b) Lineations seen in mountain ranges (orange) and dark valleys (blue). Two main trends run nearly E–W and NW–SE. (c) Rugged, overlapping mountain ranges are seen and (d) broad valleys filled with materials smooth or absorbing to Radar. (For interpretation of the references to color in this figure legend, the reader is referred to the web version of this article.)

glaciers have filled in the valley carved by a preexisting river (Marchetti, 2002). That Xanadu has such valley morphologies indicates a change in erosional and/or depositional patterns. One possibility is that the valley bottoms sunk beneath regional base level (or the mountains were uplifted), causing fluids and fluid-carried materials to accumulate in the valley bottoms. Another possibility is that increased erosion on the mountain peaks, perhaps from a stage of increased precipitation, has led to aggradation in the valleys.

Many of the widened valleys and mountain blocks have straight margins (Fig. 4b). Some of these lineations stretch for up to 100 km, and many are subparallel to one another. These patterns indicate there were regional tectonic controls on the evolution of the mountain blocks and associated river valleys. Landforms having straight margins are typical of regional extension, in this case having occurred in at least two main directions, one NE–SW and another NW–SE.

3.3. Eastern Belts

The eastern portion of Xanadu has most of the same features seen in its other areas – channels, mountains, and valleys – and many candidate impact craters (Fig. 5). The continuous unit of multiple, adjacent, mountain peaks trending over from the Middle Rugged Terrains in the west (Fig. 5a) gives way to mountain ranges in the east organized into arcuate trends of bright peaks we call belts. They are concave southward and interrupted periodically by large drainages (Fig. 5b and c).

The drainages and other river systems in the area are fairly well developed and appear to have a rectilinear, or trellis, pattern, similar to those discussed by Burr et al. (2009) in western Xanadu (Fig. 5b). The drainages are not as interconnected as those in the Western Plateaus and Drainages and are fewer in number. In addition, most drainages here are dark-floored, compared with those to the west, which are more commonly bright-floored. We conclude that there have been tectonic or structural controls on the formation or evolution of these drainages, similar to those in Burr et al. (2009). In fact, many channels trend E–W along the northern margins of the belts, which are periodically exploited by southward drainages. The N–S and E–W drainages connect, so that the overall drainage is (or was) to the south, the characteristic drainage gradient for most of Xanadu. Farther to the east, at the margin of Xanadu, river valleys appear enlarged and SAR-dark, as was seen in the Middle Rugged Terrains.

Also notable in this portion of Xanadu are six circular features listed as candidate impact craters by Wood et al. (2010). There are only nine definite impact craters and only 49 candidates identified on all of Titan. Nevertheless, more candidate craters per unit area (2.5×) are found in the eastern portion of Xanadu than elsewhere on Titan, which indicates this region may be older than the rest of Titan (Lorenz et al., 2007; Wood et al., 2007, 2010; Lopes et al., 2010).

3.4. Southern Flow Complexes

Southern Xanadu contains a variety of terrains, including basins, ridges, and interleaved, lobate flows. Since the flows dominate much of the region, we term it the Southern Flow Complexes. In the northwest part of this area is the terminus region of many of the drainages seen flowing to the south from the Western Drainages region (Section 3.1). Here, the southwestern portion of Xanadu changes abruptly from mountainous and river-carved to bland and flat (Fig. 6a). In the middle of the Southern Flow Complexes are E–W oriented mountain ranges (Fig. 6b), parallel to other E–W lineations in the area and similar to features seen on the northwestern edge of Xanadu (0°, 120°W). These could have re-

sulted from extension and rifting of mountain blocks, leading to basin-and-range style parallel block faulting. On the other hand, the confined nature of these features, the mountain spacing, and their orientation and location when compared with internal convection models led Mitri et al. (2010) to postulate that these are the result of N–S directed compression (Section 5).

At the southeastern end of Xanadu (Fig. 6c) is a region, called Hotei Regio, of interleaved, lobate, flow-like features that sit in a basin as defined by northward-flowing channels emerging from mountains at the south of Fig. 6a. These flows resemble several other regions on Titan interpreted to be the result of cryovolcanic eruptions onto the surface, such as Tui Regio, western Xanadu, and others not yet described (Barnes et al., 2006; Lopes et al., 2007, 2010; Wall et al., 2009; Soderblom et al., 2009). In this location, VIMS recorded a distinctive, 5-μm bright region (Barnes et al., 2005), which is bounded on its southern edge by the VIMS 0.94 μm bright, arcuate feature Hotei Arcus. Hotei Arcus corresponds to the SAR-bright southern mountain range (Fig. 6c, eastern star in Fig. 6a). Hotei Regio was seen to be bright at 5 μm indicating this is a region of unique composition or temperature (Wall et al., 2009; Nelson et al., 2009a). SAR stereo products reveal that the lobate features are elevated 100–200 m above surrounding terrains, typical of lava flow lobes seen in regions such as Kilauea volcano, Hawaii (Fig. 2 of Soderblom et al. (2009)).

Tui Regio, on Xanadu's southwest margin (western star, Fig. 6a), was observed by VIMS at both low and high resolution to have unique spectral characteristics, such as 5 mm brightness, and features with flow-like morphologies (Barnes et al., 2006). Observations of this region by RADAR in HiSAR mode revealed morphologies similar to the interleaved, lobate flows of Hotei Regio. In addition, an area at the west end of Xanadu, in the Western Eroded Plateaus (Fig. 3a), is the location of a purported VIMS photometrically variable region (Nelson et al., 2009b). It also has similar morphologies to the lobate flows seen in Hotei and Tui Regios and has been postulated to be the location of other, possibly recent volcanism (Wall et al., 2009). These potentially volcanic features rim the southern and western margins of Xanadu and may be related to the formation or evolution of Xanadu itself (Section 5).

4. Composition of Xanadu

Xanadu is generally bright to v-nIR instruments and SAR (Fig. 1–6), observations that are directly related to the composition and surficial layering of Xanadu. Prior to Cassini, groundbased near-IR observations (e.g., Griffith et al., 2003; Lellouch et al., 2004) had been interpreted in terms of rather simple mixtures of water ice and a darker contaminant or contaminants. It had already been pointed out, however, that the simple model of "dirty ice" with less ice and more of the dark contaminant(s) present in the darker areas was unlikely to be correct, because the 1.6 and 2.0 μm H_2O absorptions are actually stronger in the dark areas (Lorenz and Lunine, 2005). Cassini VIMS spectra of spatially resolved terrain units on Titan shed additional light on the composition, but because the surface is seen in only a small number of atmospheric windows, the result is still not a unique compositional identification. In general on Titan, materials dark to both v-nIR and SAR (the "dark brown" spectral unit that corresponds to dunes identified in the SAR images) are thought to be composed largely of organic materials precipitated out of the atmosphere in a continuous, global drizzle of photochemical debris (Soderblom et al., 2007; Lorenz et al., 2006; Lopes et al., 2010). These deposits can mask the underlying terrain to a varying degree. Areas that are dark in the v-nIR but dune-free typically appear blue in VIMS color composites because they are relatively strongly absorbing at longer wavelengths compared to the 1.3 μm band that is usually represented by blue in
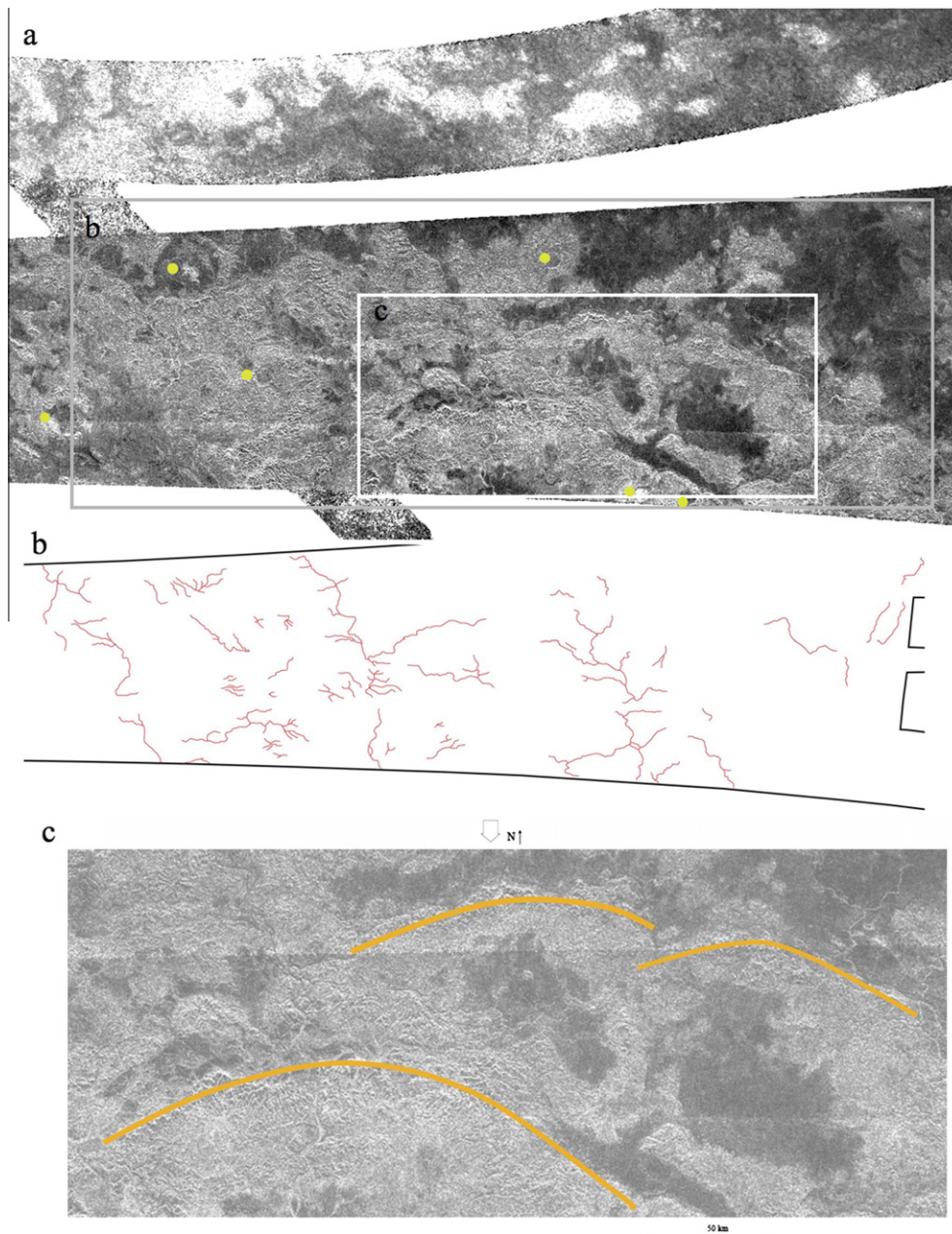
Fig. 5. (a) SAR observations of the Eastern Belts. This terrain is marked by continuous, bright, mountainous regions to the west (with impact craters) and swaths of dark, low, smooth materials to the east interspersed with mountain belts. Candidate impact crater centers marked by yellow dots. (b) Drainage traces on the eastern end of Xanadu. (c) Arcuate northern margins of mountain belts are traced. (For interpretation of the references to color in this figure legend, the reader is referred to the web version of this article.)

false-color images (Soderblom et al., 2007). Because the signal is absorbed at the H_2O bands at 1.6 and 2.0 μm, the blue material is posited to be enriched in water ice, though it is by no means pure (Soderblom et al., 2007).

Materials bright in the v-nIR are thought to be organic surface deposits, having spectral signatures consistent with little or no exposed water ice (Soderblom et al., 2007), but in contrast to the dark dunes, these deposits are probably substantially thinner. The bright surface deposits are too thin to mask or subdue relief such as the rugged mountains of Xanadu, at least at the resolution of the SAR images. Such mountains are also extremely radar-bright. This is observed in both SAR images and scatterometry data, obtained over Xanadu during the Ta and T8 passes. These data reveal a higher backscatter from Xanadu than anywhere else on Titan (Fig. 7a; Wye et al., 2007; Zebker et al., 2008; Janssen et al.,

2009). Initial modeling of these data has produced an estimated dielectric constant of 2.8–3.4 for Xanadu materials, consistent with water ice that may be slightly porous and contain a minor contaminant (Wye et al., 2008). Passive radiometric observations of Xanadu indicate a region of very low brightness temperature (Fig. 7b; Janssen et al., 2009), implying a correspondingly low emissivity, and a simple model based on polarization ratios produces an unrealistically low effective dielectric constant (~1; Fig. 7c). These observations are consistent with a water–ice layer that is extensively fractured. The surficial organic layer that hides the IR spectral signature of the ice may also play a role in inhibiting the surface reflection of microwaves.

The presence of extensive water–ice "bedrock" under the bright, non-ice surficial coating of Xanadu is also supported by theoretical considerations and perhaps by very high-resolution
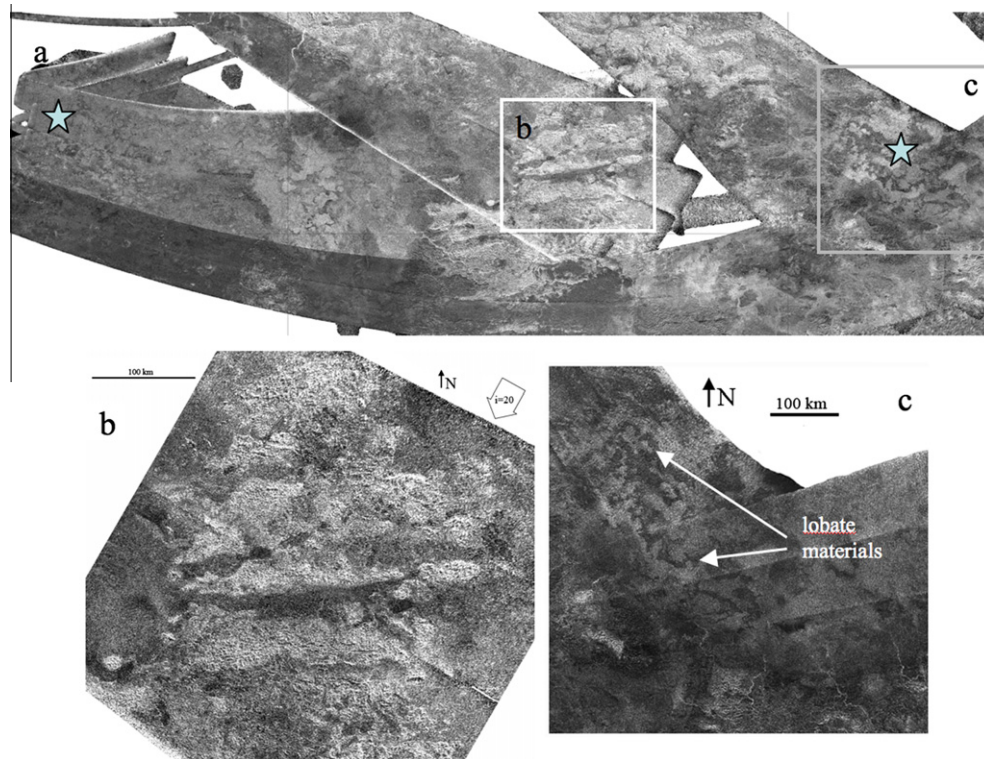
Fig. 6. (a) SAR observations of the Southern Flow Complexes. Stars indicate rough centers of VIMS 5-μm bright spot observations. (b) Sets of parallel ridges in the center may indicate N–S compression. (c) Lobate flows fill possible lowlands north of Hotei Arcus, the bright terrain at bottom.

spectral imaging. Models indicate that the interior of Titan is likely differentiated into a rocky interior, a high-pressure layer of water ice, a subsurface liquid layer and an outer ice I shell with the degree of differentiation currently under discussion (Tobie et al., 2006; Mitri and Showman, 2008; Iess et al., 2010), so the bedrock that makes up the bulk of the crust is likely to be primarily H_2O ice. VIMS observations of some mountains and channel systems in eastern Xanadu at very high spatial resolution show an admixture of the dark blue spectral unit with the bright material (Barnes et al., 2007). A possible interpretation is that enhanced fluvial erosion in these areas may partially remove atmosphere-derived organic coatings and expose the underlying water ice.

We conclude that both IR and microwave observations may be consistent with two end-member alternatives for the composition of Xanadu, with reality likely somewhere along the continuum: (1) an extensively fractured bedrock of water ice mixed with organics; and (2) an extensively fractured, pure water–ice bedrock coated by a layer of organics. Xanadu's true makeup contains materials that both dominate the IR spectral reflectance and depolarize the natural microwave emission. The thickness of the organic layer or mixture is rather poorly constrained. Its minimum thickness is a few microns, at least in patches, because it is visible to VIMS (Soderblom et al., 2007). If the surface is smooth, a graded-density porous layer at least a centimeter or so thick must be present to depolarize emitted microwaves, but the organic material may or may not be part of this layer. If the organic layer is purely a coating, its maximum thickness is limited to at most a few meters by its probably small but finite microwave absorptivity that hides the volume-scattering layer beneath. If the organic layer contributes to the volume scattering, then it could be thicker, but in any case must be less than ∼100 m thick because it does not mask the bedrock geology at the resolution of the SAR images, assuming valleys, peaks, and ridges are best formed and maintained in water ice bedrock, and not in organic layers. More extensive modeling of volume scat-

tering is required to put a better constraint on Xanadu's near-surface composition and structure.

5. Topography and elevation of Xanadu

Studies of the topography of Xanadu, both on a local and regional scale, are underway (e.g., Radebaugh et al., 2007; Stiles et al., 2009; Kirk and Radebaugh, 2007). Over distances less than 50 km, we can apply the technique of 1-D radarclinometry, or shape-from-shading, to determine slopes and heights of individual mountains (Kirk et al., 2005; Radebaugh et al., 2007). We utilize a cos(incidence angle) function based on observations of the incidence-angle dependence of Xanadu itself and of isolated mountains of similar morphology elsewhere on Titan. This diffuse scattering law is consistent with the enhanced volume scattering inferred from radiometry of Xanadu and the highly scattering nature expected from fractured bedrock as discussed above. With this assumption, relatively typical mountains within Xanadu are found to have some slopes >30° and heights just over 2000 m (Radebaugh et al., 2007) when corrected for the limited resolution of the images (Kirk and Radebaugh, 2007).

In this paper, we also present for the first time digital terrain models (DTMs) of portions of Xanadu, again derived using the cos(incidence angle) backscatter model. The 2-D radarclinometry/photoclinometry algorithm described by Kirk (1987) and Kirk et al. (2003) was used; it is only applicable in areas (as in parts of Xanadu) where the radar-scattering properties are uniform over extended distances. To further reduce the distortions of the DTM that would result from including both bright (mountainous) and dark (valley fill) areas in the analysis, we highpass filtered the image to remove variations in average scattering over distances larger than 10 km. Kirk (1987) showed that reconstructing a surface from a highpass-filtered image yields an equivalently highpass-filtered version of the topography, plus at most minor distortions. SARTopo
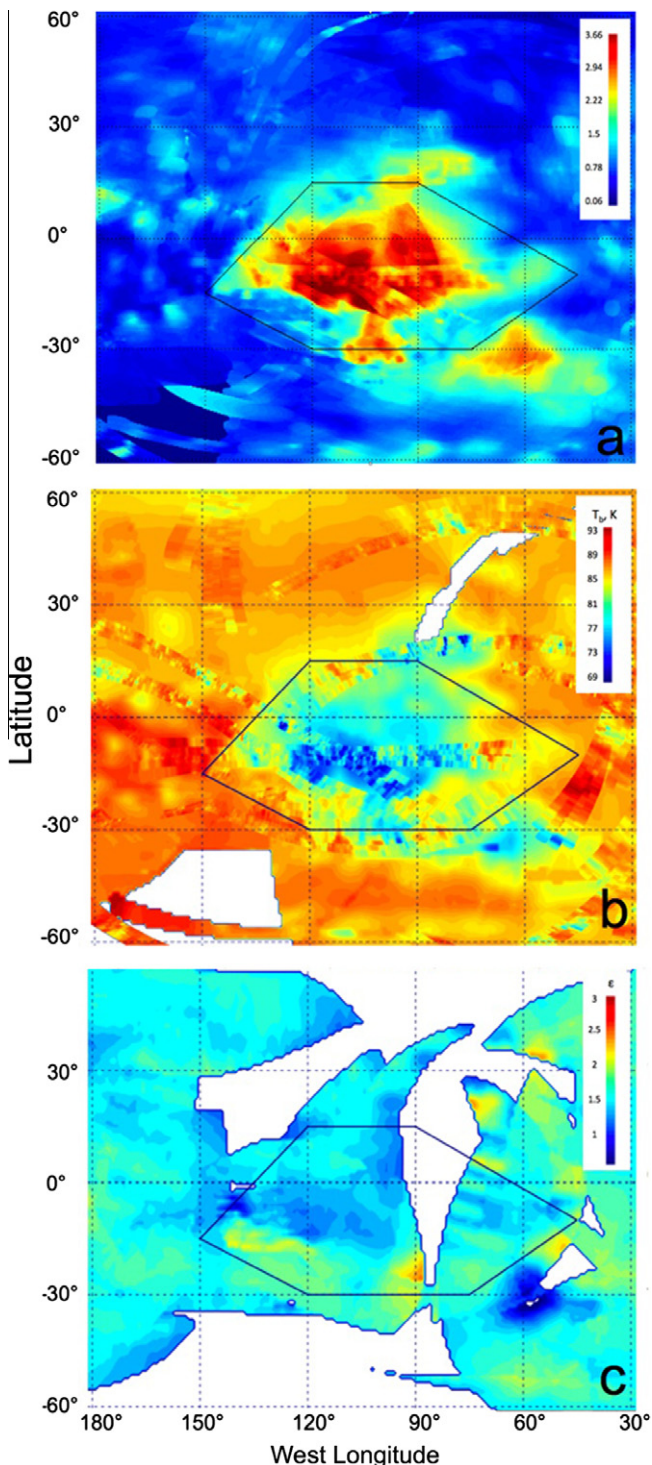
Fig. 7. (a) Scatterometry map of Xanadu showing real-aperture backscatter cross sections normalized for incidence-angle effects; the values plotted are the ratio residuals to the best-fit model for the average Titan surface (as in Wye et al. (2007)). Dark red indicates high backscatter in the Xanadu region. (b) Brightness temperature mosaic at normal incidence of the Xanadu region from radiometry observations (from Janssen et al. (2009)). Note the regionally low brightness temperature of the Xanadu region. (c) Effective dielectric constant in Xanadu (based on the polarized thermal emission, Janssen et al., 2009). A particularly sharp linear boundary is observed along the southwestern border.

(Stiles et al., 2009) and stereo (Kirk et al., submitted for publication) give a complimentary view of the relief of Xanadu lowpass-filtered at a scale of ten to a few tens of kilometers, and are discussed below. The resulting DTMs (Fig. 8) thus indicate relative

relief for features smaller than about 10 km, but not absolute relief. The results show heights for individual mountains on the order of 500 m in many places, but also an asymmetry between RADAR-facing and away-facing slopes that is indicative of resolution effects (Kirk and Radebaugh, 2007). After correcting the data for resolution effects, these mountains have heights between 1000 and 2000 m, consistent with the 1-D radarclinometry profiles. The advantage of the DTMs is that they show in planimetric form the characteristics of the terrain in different locations across Xanadu (Fig. 8). Features such as plateaus, wide valley, and steep summits as observed morphologically in SAR images are corroborated by the DTMs, which provide additional elevation information.

Xanadu's regional elevation, overall lower than surrounding terrains, and decreasing gently from west to east (Zebker et al., 2009; Stiles et al., 2009) is perhaps the most puzzling aspect of its character. An early speculation (Griffith et al., 1991; Lorenz, 1993) was that bright regions on Titan might be kept bright (against a supposed global and continuous drizzle of presumed dark photochemical debris) by methane rainfall washing this dark material into the lowlands. The undersaturation of Titan's lower atmosphere implied that raindrops might evaporate during descent and thus highland areas would naturally receive more rainfall (Lorenz, 1993). Xanadu's lack of large-scale positive relief (Zebker et al., 2009; Stiles et al., 2009) erodes this paradigm. On the other hand, more detailed microphysical modeling, including the role of ethane and of evaporative cooling in raindrops (Graves et al., 2008), shows that raindrops can reach lowland surfaces on Titan in any case, as indeed the presence of river channels all over Titan's surface suggests they must, at least at some time in the past.

Initial Cassini data suggested Xanadu was elevated above surrounding terrains because (a) it is bright both in the n-IR and in SAR, and smaller bright terrains elsewhere on Titan are generally elevated above dark terrains; (b) river channels on the east and south of Xanadu appear to flow away from the margin of Xanadu, from mountainous regions to lowlands (Barnes et al., 2007); and (c) adjacent dunes appear to be diverting around Xanadu, typical of dune behavior around elevated topography (Lorenz et al., 2006). Specifically, the dune orientations in Shangri-La to the west of Xanadu veer sharply southwards as they approach the Xanadu margin, suggesting that the winds are topographically diverted regionally (Radebaugh et al., 2008).

However, RADAR-derived topography shows that Xanadu is not elevated above surrounding terrains, at least in the mean. Both SARTopo swaths (Stiles et al., 2009) and altimetric traces (Zebker et al., 2009) across Xanadu range from zero to negative 1 km regional elevation relative to Titan's mean radius of 2575 km (Fig. 9), decreasing gently from west to east, also decreasing somewhat from north to south. It should be noted that these observations are resolution-limited, so that each measurement is an average over a footprint several tens of km in size, larger than the typical mountain ranges and valleys. It is thus the mean elevation that is described above; peaks are higher and valleys lower. The presence of peaks indicates the region was relatively elevated and exposed to erosional processes, likely for long time scales, given the degree of erosion of the rugged terrains. In addition, many channels in western Xanadu appear to drain to the south of Xanadu, as if from highlands to lowlands; yet central Xanadu now appears to be depressed compared with its surroundings. How can we explain these discrepancies?

The solution is likely tectonic and/or erosional in nature. Xanadu appears to have undergone a loss of elevation since its formation, perhaps through a combination of regional erosion, relaxation, or subsidence along region-bounding faults (see Section 6). Regarding relaxation, Mitri et al. (2010) show that mountains on Titan experience moderate viscous relaxation over 10^8–10^9 year. Subsidence along faults is explored in Section 6.
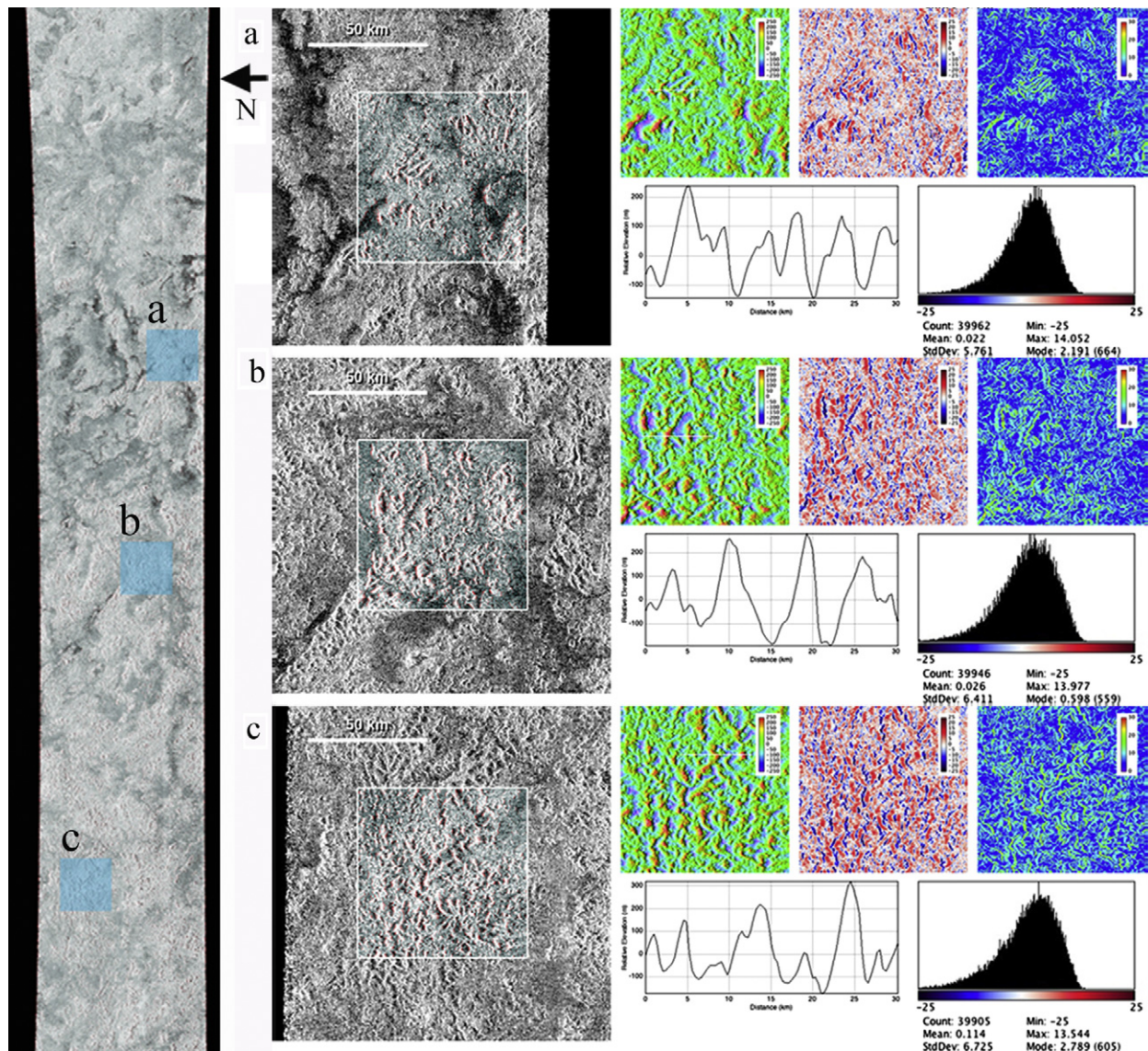
Fig. 8. Digital Topographic Models (DTMs) of selected parts of Xanadu. 2-D radarclinometry was used to produce a DTM of the entire area shown in the context SAR image at left (latitudes 13–7°S, longitudes 70–140°W), after highpass filtering to reduce the effects of backscatter variations. Boxes in the context image show the locations of subareas presented at right, chosen to illustrate a range of mountain morphologies with a relatively small influence from intrinsically darker intermountain fill, which leads to artifacts in the DTM. For each region, a synthetic stereo anaglyph is shown, along with a color-coded elevation map with relief shading, a map of bidirectional (north–south) slopes, a map of adirectional (downhill) slopes, a histogram of bidirectional slopes, and a representative topographic profile extracted from the DTM at a location marked in the elevation map. The asymmetry between radar-facing (north) and away-facing (south) slopes, particularly evident in the profiles and slope histograms, is a clear indication that the DTM has been distorted by the limited resolution of the image. Some elevation differences nevertheless reach ~500 m from local peak to valley and would correspond to >1000 m of relief when corrected for the limited resolution of the image. North is to the left in all images. Regions were selected across Xanadu to include samples from the Middle Rugged Terrains (a and b) and the Western Plateaus (c).

The overall relief of Xanadu is not large, yet the terrain is rugged. Therefore, dunes may be obstructed by their first encounter with locally elevated landforms, even at very low elevations, and then dunes do not progress beyond this obstacle. Another possible explanation is meteorological in origin. Xanadu may act as a "source" for flow, in that overall radiative cooling by high albedo or small-scale katabatic slope-driven winds generate a net flow away from Xanadu. Tokano (2008) has attempted to reproduce the observed dune orientation field with a global circulation model (GCM), with various perturbations (such as defining Xanadu as a plateau) so far with limited success. Xanadu may also be a significant local perturber of weather – Adamkovics et al. (2007) have reported groundbased evidence that a drizzle presently falls over much of Xanadu, although other observations (Kim et al., 2008) seem to refute this finding. Transient tropospheric clouds have been occasionally observed over southern Xanadu (Schaller et al.,

2009) and near its southern boundary (Roe et al., 2005; Griffith et al., 2005).

6. Xanadu formation and evolution scenario

A formation model for Xanadu must account for all observed aspects of its current and inferred past geology and morphology. Major characteristics to be explained by such a model include the presence of (a) terrains made rugged through exposure to erosion by rainfall; (b) ancient terrains with extensive and evolved river systems and likely impact craters that have not been buried or modified beyond recognition; (c) a regional southward gradient as indicated by river drainage directions and SARTopo results; (d) organization of materials into tectonically governed mountain ranges and valley floors; and (e) probable volcanic regions at the southern and western margins of Xanadu.
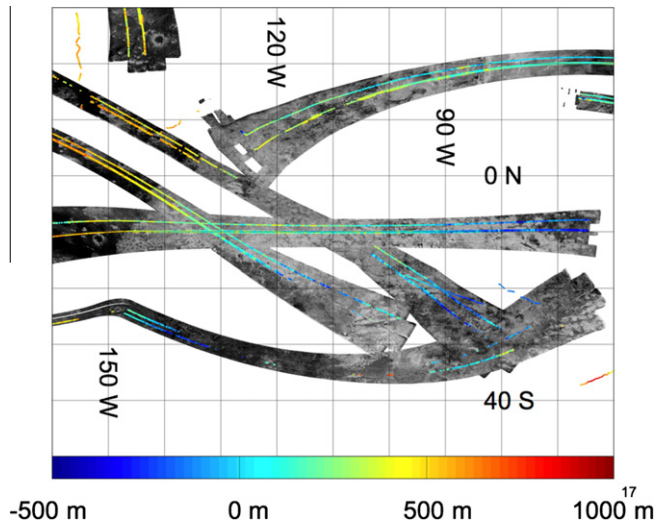
Fig. 9. SARTopo data across Xanadu. SARTopo traces are obtained as lines that parallel the RADAR track, and there are typically two per swath. Note that there is a gentle decrease in elevation between the Shangri-La dune field to the west of Xanadu and the western boundary of Xanadu and a regional E–SE gradient throughout Xanadu. From Stiles et al. (2009).

compression from north to south directed forces, followed by NE–SW and NNW–SSE directed extension, with crustal thinning and basin formation, and downdropping along marginal faults, which also serve as pathways for magma ascent and eruption, all with concurrent erosion by methane rainfall (Fig. 10).

We propose that early in Titan's history the Xanadu region underwent crustal thickening, resulting in high-standing terrain that has been exposed to fluvial/pluvial erosion and impact cratering for up to 2 byr (Lorenz et al., 2007 derive a crater exposure age for Titan of up to 1 Gyr, and Wood et al. (2010) note that Xanadu has roughly double the Titan average cratering density). In our model, this thickening occurs via regional, N–S directed compression (Fig. 10a). The compression created the mountainous terrains of the Middle Rugged Terrains, the thrust-sheet-produced, arcuate mountain belts in the Eastern Belts, and the E–W oriented parallel ridges at the south end of Xanadu (T44, Fig. 6b) in the Southern Flow Complexes. The rugged terrain is similar to regions on Earth formed by compressional tectonics (like the Himalayas, see Radeb-augh et al., 2007) that have been modified by rainfall erosion concentrated along their exposed summits. The arcuate mountain belts in eastern Xanadu bear the morphology of thrust belts, wherein a crustal block overrides adjacent substrate, as a result, in this case, of N–S compressive forces. The parallel ridges in the Southern Flow Complexes are similar to the E–W trending mountain chains at the east end of the Belet sand sea (~210°W longitude) and others at the northern edge (~140°W longitude) and southeastern edge (~60°W longitude) of Xanadu. All of these have
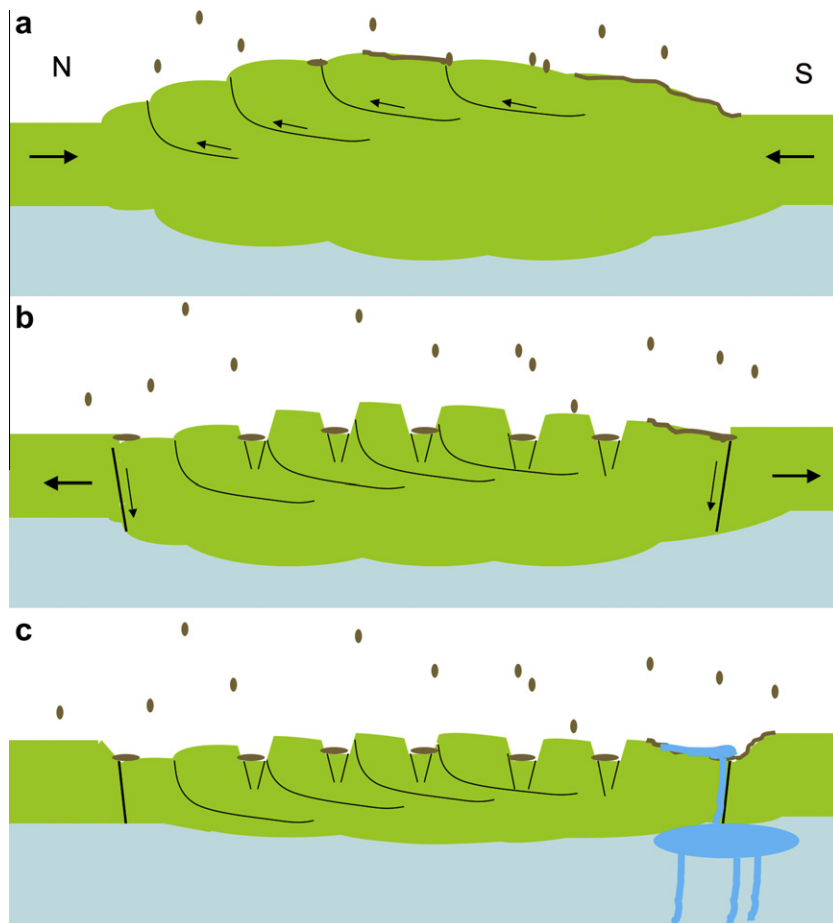
With these observations in mind, we present a model for Xanadu's formation that includes crustal thickening through regional

Fig. 10. Model for formation and evolution of Xanadu. (a) Regional N–S directed compression results in thrust belts, with offset crust bounded by the curved lines, and lithospheric thickening. Methane rainfall establishes drainages that flow preferentially to the south as a result of a regional slope. (b) Regional extension creates horst and graben terrain, causes downdropping along Xanadu-bordering faults, and initiates crustal thinning. Meteoric fluids fill the basins. (c) Erosion continues the process of crustal thinning as isostasy is maintained. Region-bounding faults created by extension provide pathways for cryomagma ascent.

been modeled as long-wavelength lithospheric compressional folds (Mitri et al., 2010). Compression on Titan can be straightforwardly explained as the progressive cooling with time of Titan's interior resulting from partial freezing of a subsurface water ocean (or water with ammonia or other antifreezes) leading to global radial contraction and shortening of the lithosphere (Mitri et al., 2010). Mitri et al., have shown that contractional crustal deformation of the ice I shell can produce topographic heights of several kilometers for high temperature gradients in the ice shell (order of 10 K km^{-1}), corresponding to an ancient high heat flux from the interior. Tectonism driven by global volume contraction could even cause ammonia–water pockets close to neutral buoyancy within the ice shell to erupt effusively onto the surface (Mitri et al., 2008).

Contraction of the Xanadu region would likely entail thickening of the crust downward into Titan's mantle as well as uplift, in order to maintain isostasy. Recent results for Titan's shape predict topographic features on Titan should be well compensated (Zebker et al., 2009; Iess et al., 2010).

Subsequently, a stage of extension (Fig. 10.b) directed NE–SW and NW–SE (with neither trend obviously preceding the other) created the linear valleys seen in the Eastern Belts terrain and elsewhere in Xanadu (Paganelli et al., 2010). This extension resulted in a decrease in elevation of the basins, crustal thinning as isostasy is maintained, and a return of sublithospheric mantle material, as in for example the western US Basin and Range (Fig. 10b). Part of this extension could be accommodated locally and fairly shallowly in the form of fault block failure of elevated terrains, examined through numerical modeling by Koons (1987), and meshing well with predictions for ice rock failure at thicknesses over several kilometers (Renshaw and Schulson, 2001).

This regional extension and mountain block failure resulted in a reduction of Xanadu's overall elevation. We suggest this process was accentuated by concurrent downdropping along faults bordering Xanadu, leading to a regional reduction in elevation below that of surrounding terrains as corroborated by SARTopo and global altimetry measurements (Fig. 10c).

Erosion through methane rainfall has acted throughout Xanadu's history to bring down summit elevations and create vast, integrated river valleys and eroded terrains. A regional southward gradient to the Xanadu region, perhaps related to asymmetry in the early thrust belts, or of an unknown cause, has led to dominantly southward drainages. Given the maturity of Xanadu's river networks compared to other regions on Titan, this regional gradient must have persisted since early in Xanadu's history.

We hypothesize that fracture zones bordering Xanadu accommodated some of the downward slip (accommodation also occurred by viscous relaxation) of the Xanadu province. These fractures also acted as cryomagma pathways, leading to the eruption of cryovolcanic materials in the locations of Hotei, Tui Regio, and western Xanadu (Fig. 10d). The southwest boundary of Xanadu contains an unusually sharp linear boundary in the measured backscatter, radiometry, and effective dielectric constant retrieved from the polarization of the radiometry (Fig. 7; Janssen et al., 2009). Such a feature is consistent with an abrupt change in surface properties resulting from such a faulting process.

This model for the formation and evolution of Xanadu is necessarily simple at this early stage of data analysis of the Xanadu region, and will evolve with the inclusion of new data and numerical modeling of materials and processes. The model incorporates the elements that correlate best with current observations of Xanadu.

7. Discussion and conclusions

The Xanadu province remains one of the most intriguing regions on Titan, in terms of the variety of geologic morphologies

and processes and complexity of its history. As a first attempt at a regional geomorphological classification of the various terrains within Xanadu, we find it is broadly comprised of Western Drainages, consisting of evolved river systems and possible cryovolcanic regions; Middle Rugged Terrains, with mountainous terrains interspersed with valleys; Eastern Belts, with arcuate mountain belts, broad, smooth valleys, and many candidate impact craters; and Southern Flow Complexes, containing possible cryovolcanic terrains, possible fold-thrust belts, and drainages. These geographical distinctions enable a preliminary model for the geological history of Xanadu.

This evolutional history we propose for Xanadu begins with a N–S oriented, equatorial compression (Mitri et al., 2010) that caused lithospheric thickening and produced extensive, rugged mountain ranges and large-scale folds, expressed as parallel ridges and fold-thrust belts. Subsequently, extension occurred, leading to lineations exposed in horst-and-graben-like mountains and valleys. It is possible this tectonic compression and extension occurred elsewhere on Titan but has been partly obscured by sand sea or organic precipitate sedimentation or by methane rainfall erosion. There is some evidence of regional tectonic controls on river drainages at Titan's north polar regions (Porco et al., 2005; Radebaugh et al., 2009).

In order to account for the observed low regional elevations of Xanadu compared to surrounding terrains, we postulate that Xanadu experienced ongoing erosion and downdropping along region-bounding faults. The faults were exploited by cryovolcanic materials that ascended and erupted along the southern and western margin of Xanadu, perhaps relatively recently. Thus, Xanadu may be an old, eroded terrain undergoing change through fluvial action and internal activity.

Fluvial erosion might be responsible for removing the deposition of hydrocarbons and nitriles associated with methane photolysis that occurred over billions of years (Yung et al., 1984). Xanadu must have somehow preserved a coating of organics thick enough to inhibit the spectral signature of water and to prevent surface reflection of microwaves, but thin enough not to mask the topography or absorb microwaves. If Xanadu became tectonically quiescent not long after the core convective events led to compression, followed by extension, then two billion years of photolysis would have covered Xanadu with tens of meters depth of photochemical debris.

Did this proposed sequence of events occur only in Xanadu? If a province like Xanadu formed elsewhere on Titan, we have little evidence for it. Mountainous terrains across Titan resemble Xanadu in radiometric character; perhaps Xanadu is the only region not enough obscured by organic deposits to reveal its underlying character and history. Xanadu's uniqueness and location are perhaps related to global processes. Titan's first global shape model has ellipsoid maxima ~90° away from Xanadu (Zebker et al., 2009). In addition, Xanadu is located directly on the center of Titan's leading hemisphere. These observations may indicate a major, singular event was associated with Xanadu's formation, but whether tidal, tectonic, or impact-related remains uncertain pending regional-scale altimetric data, higher imaging resolution, and subsurface sounding – all of which except perhaps the first require a future mission to unravel.

authors also acknowledge the thorough and helpful reviews from Geoffrey Collins and Devon Burr.

References

Adamkovics, M., Wong, M.H., Laver, C., de Pater, I., 2007. Widespread morning drizzle on Titan. Science 318, 962–965.

Barnes, J.W. et al., 2005. A 5-Micron-bright spot on Titan: Evidence for surface diversity. Science 310, 92–95. doi:10.1126/science.1117075.

Barnes, J.W. et al., 2006. Cassini observations of flow-like features in western Tui Regio, Titan. Geophys. Res. Lett. 33, L16204. doi:10.1029/2006GL026843.

Barnes, J. et al., 2007. Near-infrared spectral mapping of Titan's mountains and channels. J. Geophys. Res. 112, E11006. doi:10.1029/2007JE002932.

Baugh, N.F., 2008. Fluvial Channels on Titan. MS Thesis, University of Arizona, Tucson, 45pp.

Blom, R.G., 1988. Effects of variation in incidence angle and wavelength in radar images of volcanic and aeolian terranes, or now you see it, now you don't. Int. J. Rem. Sens. 9, 945–965.

Burr, D.M., Jacobsen, R.E., Roth, D.L., Phillips, C.B., Mitchell, K.L., Viola, D., 2009. Fluvial network analysis on Titan: Evidence for subsurface structures and west-to-east wind flow, southwestern Xanadu. Geophys. Res. Lett. 36. doi:10.1029/2009GL040909.

Campbell, D.B., Black, G.J., Carter, L.M., Ostro, S.J., 2003. Radar evidence for liquid surfaces on Titan. Science 302, 431–434. doi:10.1126/science.1088969.

Combes, M., Vapillon, L., Gendron, E., Coustenis, A., Lai, O., Wittemberg, R., Sirdey, R., 1997. Spatially-resolved images of Titan by means of adaptive optics. Icarus 129, 482–497.

Elachi, C. et al., 2005. Cassini Radar views the surface of Titan. Science 308, 970–974. doi:10.1126/science.1109919.

Graves, S.D.B., McKay, C.P., Griffith, C.A., Ferri, F., Fulchignoni, M., 2008. Rain and hail can reach the surface of Titan. Planet. Space Sci. 56, 346–357.

Griffith, C.A., Owen, T.C., Wagener, R., 1991. Titan's surface and troposphere, investigated with ground-based, near-infrared observations. Icarus 93, 362–378.

Griffith, C.A., Owen, T., Geballe, T.R., Rayner, J., Rannou, P., 2003. Evidence for the exposure of water ice on Titan's surface. Science 300, 628–630.

Griffith, C.A. et al., 2005. The evolution of Titan's mid-latitude clouds. Science 310, 474–477.

Iess, L., Rappaport, N.J., Jacobson, R.A., Racioppa, P., Stevenson, D.J., Tortora, P., Armstrong, J.W., Asmar, S.W., 2010. Gravity field, shape, and moment of inertia of Titan. Science 327, 1367–1369.

Janssen, M.A., et al., and the Cassini Radar Team, 2009. Titan's surface at 2.2-cm wavelength imaged by the Cassini RADAR radiometer: Calibration and first results. Icarus. doi:10.1016/j.icarus.2008.10.017.

Janssen, M.A., Le Gall, A., Wye, L.C. Anomalous radar backscatter from Titan's surface. Icarus, submitted for publication.

Kim, S.J., Trafton, L.M., Geballe, T.R., 2008. No evidence of morning or large-scale drizzle on Titan. Astrophys. J. 679, L53–L56. doi:10.1086/588839.

Kirk, R.L., 1987. A Fast Finite-Element Algorithm for Two-Dimensional Photoclinometry. Ph.D. Thesis, Part III, California Institute of Technology, Pasadena, CA, pp. 165–258.

Kirk, R.L., Radebaugh, J., 2007. Resolution effects in radarclinometry. In: ISPRS Working Group IV/7 Workshop "Advances in Planetary Mapping 2007", Houston, March 2007. <http://www.dlr.de/pf/Portaldata/6/Resources/dokumente/isprs_2007/Kirk_3__ISPRS_2007.pdf>.

Kirk, R.L., Barrett, J.M., Soderblom, L.A., 2003. Photoclinometry made simple…? In: ISPRS Working Group IV/9 Workshop "Advances in Planetary Mapping 2003", Houston, March 2003. <http://astrogeology.usgs.gov/Projects/ISPRS/Meetings/Houston2003/abstracts/Kirk_isprs_mar03.pdf>.

Kirk, R.L., Callahan, P., Seu, R., Lorenz, R.D., Paganelli, F., Lopes, R.M., Elachi, C., and the Cassini Radar Team, 2005. Radar reveals Titan topography. Lunar. Planet. Sci. XXXVI, 2227 (abstract).

Kirk, R.L., Wall, S.D., Lorenz, R.D., Lunine, J.I., Radebaugh, J., Soderblom, L.A., Stiles, B.W., Janssen, M.A., Paganelli, F., Lopes, R., and the Cassini RADAR Team, 2006. A high resolution view of the Xanadu region of Titan from The Cassini RADAR. Bull. Am. Astron. Soc. 38, 52.03 (abstract).

Kirk, R.L., et al., and the Cassini RADAR Team. Three-dimensional views of Titan's diverse surface features from Cassini RADAR stereogrammetry. Icarus, submitted for publication.

Koons, P.O., 1987. Some thermal and mechanical consequences of rapid uplift: An example from the Southern Alps, New Zealand. Earth Planet. Sci. Lett. 86, 307–319.

Lellouch, E., Schmitt, B., Coustenis, A., Cuby, J.-G., 2004. Titan's 5-micron lightcurve. Icarus 168, 209–214.

Lemmon, M.T., Karkoschka, E., Tomasko, M., 1993. Titan's rotation – Surface feature observed. Icarus 103, 329–332. doi:10.1006/icar.1993.1074.

Lemmon, M.T., Karkoschka, E., Tomasko, M., 1995. Titan's rotational light-curve. Icarus 113, 27–38. doi:10.1006/icar.1995.1003.

Lopes, R.M.C. et al., 2007. Cryovolcanic features on Titan's surface as revealed by the Cassini Titan Radar Mapper. Icarus 186, 395–412.

Lopes, R.M.C. et al., and the Cassini RADAR Team, 2010. Distribution and interplay of geologic processes on Titan from Cassini Radar data. Icarus 205, 540–558. doi:10.1016/j.icarus.2009.08.010.

Lorenz, R.D., 1993. The life, death and afterlife of a raindrop on Titan. Planet. Space Sci. 41, 647–655.

Lorenz, R.D., Lunine, J.I., 2005. Titan's surface before Cassini. Planet. Space Sci. 53, 557–576.

Lorenz, R.D. et al., 2006. The Sand Seas of Titan: Cassini RADAR observations of longitudinal dunes. Science 312, 724–727.

Lorenz, R.D. et al., and the Cassini RADAR Team, 2007. Titan's young surface: Initial impact crater survey by Cassini RADAR and model comparison. Geophys. Res. Lett. 34, L07204. doi:10.1029/2006GL028971.

Lorenz, R.D. et al., 2008. Fluvial channels on Titan: Initial Cassini RADAR observations. Planet. Space Sci. 56, 1132–1144.

Malaska, M., Radebaugh, J., Lorenz, R., Mitchell, K., Farr, T., Stofan, E., 2010. Identification of karst-like terrain on Titan from valley analysis. Lunar Planet. Sci. XLI. Abstract 1544.

Marchetti, M., 2002. Environmental changes in the central Po Plain (northern Italy) due to fluvial modifications and anthropogenic activities. Geomorphology 44, 361–373.

Meier, R., Smith, B.A., Owen, T.C., Terrile, R.J., 2000. The surface of Titan from NICMOS observations with the Hubble Space Telescope. Icarus 145, 462–473.

Mitri, G., Showman, A.P., 2008. Thermal convection in ice-I shells of Titan and Enceladus. Icarus 193, 387–396. doi:10.1016/j.icarus.2007.07.016.

Mitri, G., Showman, A.P., Lunine, J.I., Lopes, R.M.C., 2008. Resurfacing of Titan by ammonia–water cryomagma. Icarus 196, 216–224. doi:10.1016/j.icarus.2008.02.024.

Mitri, G., Bland, M.T., Showman, A.P., Radebaugh, J., Lopes, R.M.C., Lunine, J.I., Pappalardo, R.T., and the Cassini Radar Team, 2010. Mountains on Titan. J. Geophys. Res., in press. doi:10.1029/2010JE003592.

Nelson, R.M. et al., 2009a. Saturn's Titan: Surface change, ammonia, and implications for atmospheric and tectonic activity. Icarus 199, 429–441. doi:10.1016/j.icarus.2008.08.013.

Nelson, R.M. et al., 2009b. Photometric changes on Saturn's Titan: Evidence for active cryovolcanism. Geophys. Res. Lett.. doi:10.1029/2008GL036206.

Noll, K.S., Knacke, R.F., 1993. Titan – 1.5 micron photometry spectrophotometry and a search for variability. Icarus 101, 272–281. doi:10.1006/icar.1993.1024.

Paganelli, F., Pappalardo, R., Schubert, G., Stiles, B., Collins, G.C., Mitchell, K., Stofan, E., 2010. Preliminary analysis of structural elements of Titan and implications for stress. Lunar. Planet. Sci. XXXXI, 2664 (abstract).

Porco, C.C. et al., 2005. Imaging of Titan from the Cassini spacecraft. Nature 434, 159–168. doi:10.1038/nature03436.

Radebaugh, J., Lorenz, R.D., Kirk, R.L., Lunine, J.I., Stofan, E.R., Lopes, R.M.C., Wall, S.D., 2007. Mountains on Titan observed by Cassini Radar. Icarus 192, 77–91. doi:10.1016/j.icarus.2007.06.020.

Radebaugh, J., et al., 2008. Dunes on Titan observed by Cassini Radar. Icarus 194, 690–703. doi:10.1016/j.icarus.2007.10.015.

Radebaugh, J., et al., and the Cassini RADAR Team, 2009. Fluvial Erosion on Titan: Scales and Landform Modification. AAS/Division for Planetary Sciences Meeting 41, #36.07.

Renshaw, C.E., Schulson, E.M., 2001. Universal behaviour in compressive failure of brittle materials. Nature 412, 897–900.

Richardson, J., McEwen, A.S., Lorenz, R.D., 2004. Titan's surface and rotation – New insights from Voyager images. Icarus 170, 113–124.

Roe, H.G., Brown, M.E., Schaller, E.L., Bouchez, A.H., Trujillo, C.A., 2005. Geographic control of Titan's mid-latitude clouds. Science 310, 477–479.

Schaller, E.L., Roe, H.G., Schneider, T., Brown, M.E., 2009. Storms in the tropics of Titan. Nature 460, 873–875.

Smith, P.H., Lemmon, M.T., Lorenz, R.D., Sromovsky, L.A., Caldwell, J.J., Allison, M.D., 1996. Titan's surface, revealed by HST imaging. Icarus 119, 336–339.

Soderblom, L. et al., 2007. Correlations between Cassini VIMS spectra and RADAR SAR images: Implications for Titan's surface composition and the character of the Huygens Probe landing site. Planet. Space Sci. 55, 2025–2036.

Soderblom, L.A. et al., 2009. The geology of Hotei Regio, Titan: Correlation of Cassini VIMS and RADAR. Icarus 204, 610–618.

Stiles, B.W. et al., and the Cassini RADAR Team, 2009. Determining Titan surface topography from Cassini SAR data. Icarus 202, 584–598.

Stofan, E.R. et al., 2007. The lakes of Titan. Nature 445, 61–64. doi:10.1038/nature05438.

Tobie, G., Lunine, J.I., Sotin, C., 2006. Episodic outgassing as the origin of methane on Saturn's moon Titan. Nature 440, 61–64.

Tokano, T., 2008. Dune-forming winds on Titan and the influence of topography. Icarus 194, 243–262. doi:10.1016/j.icarus.2007.10.007.

Ulaby, Moore., Fung, 1981. Microwave Remote Sensing: Active and Passive, Vol. 1: Microwave Remote Sensing Fundamentals and Radiometry. Addison-Wesley Publishing Company, Inc., Reading, MA.

Wall, S.D. et al., 2009. Cassini RADAR images at Hotei Arcus and western Xanadu, Titan: Evidence for geologically recent cryovolcanic activity. Geophys. Res. Lett., 36. doi:10.1029/2008GL036415.

Williams, D.A., Radebaugh, J., Keszthelyi, L.P., McEwen, A.S., Lopes, R., Doute, S., Greeley, R., 2002. Geologic mapping of the Chaac-Camaxtli region of Io from Galileo imaging data. J. Geophys. Res. 107. doi:10.1029/2001JE001821.

Wood, C., Kirk, R.L., Stofan, E.R., Stiles, B., Zebker, H., Ostro, S., Radebaugh, J., Lorenz, R.D., Callahan, P., Wall, S., 2007. Xanadu is old, rugged and low-lying. Bull. Am. Astron. Soc. 38, 500.

Wood, C.A., Lorenz, R.D., Kirk, R.L., Lopes, R.M.C., Mitchell, K., Stofan, E.R., and the Cassini RADAR Team, 2010. Impact craters on Titan. Icarus 206, 334–344.

Wye, L.C., Zebker, H.A., Ostro, S.J., West, R.D., Gim, Y., Lorenz, R.D., and The Cassini Radar Team, 2007. Electrical properties of Titan's surface from Cassini RADAR scatterometer measurements. Icarus 188, 367–385. doi:10.1016/j.icarus.2006.12.008.

Wye, L.C., Zebker, H.A., Lopes, R.M., Peckyno, R., Le Gall, A., Janssen, M.A. 2008. Surface parameters of Titan feature classes from Cassini RADAR backscatter measurements. Eos, Trans., AGU (Fall Suppl.). Abstract P21A-1318.

Yung, Y.L., Allen, M., Pinto, J.P., 1984. Photochemistry of the atmosphere of Titan – Comparison between model and observations. Astrophys. J. Suppl. Ser. 55, 465–506.

Zebker, H.A., Wye, L.C., Janssen, M.A., and the Cassini Radar Team, 2008. Titan's surface from reconciled Cassini microwave reflectivity and emissivity observations. Icarus 194, 704–710.

Zebker, H.A., Stiles, B., Hensley, S., Lorenz, R., Kirk, R.L., Lunine, J., 2009. Size and shape of Saturn's moon Titan. Science 324, 921–923.